Propagating waves observed in a bistable oscillator array

Kuniyasu SHIMIZU†

†Dept. of Electrical, Electronics and Computer Engineering, Chiba Institute of Technology, Japan
2-17-1, Tsudanuma, Narashino, Chiba 275-0016, Japan

Email: kuniyasu.shimizu@it-chiba.ac.jp

Abstract—This study deals with a propagating wave observed in a bistable oscillator array, consisting of an LC resonator and a nonlinear conductance. The voltage-current characteristic of the nonlinear conductance is described by a fifth-order polynomial function, and this characteristic curve plays a role in the observation of propagating waves. This study performs an examination for the circuit implementation of the coupled bistable oscillators. By using a circuit simulator, we assume two different nonlinear conductances, and the influence on dynamics of the propagating waves are investigated. Furthermore, the simulated characteristics are compared with the numerical results. In addition, we report experimental observations of the several propagating waves.

1. Introduction

Intrinsic localized modes (ILMs) in a nonlinear lattice system has attracted intensive research interest in recent years [1, 2]. The ILMs are investigated in various lattice systems numerically and experimentally. The nonlinear phenomena is assumed to have a wide field of application, one of which is measuring field using micro-mechanical cantilever array [2].

It has been known that complex propagating waves, where a spatio-temporally localized excitation propagates in one direction with constant speed, emerge in a coupled bistable oscillator system [3, 4]. The individual oscillator is a simple circuit, which consists of one inductor, one capacitor, and one nonlinear conductance. These propagating waves have been numerically investigated in detail, especially with regard to their initiating mechanisms. In addition, the laboratory experiment is also possible, which allows us to observe propagating waves and compare them with numerical results using standard electrical instruments and off-the-shelf components [5]. However, some of the numerically obtained propagating waves have not been observed so far.

Addressing the subject, this study is aimed to perform an examination for the circuit implementation of the coupled bistable oscillators. By using the circuit simulator LTSPICE, we assume two different nonlinear conductances, and the influence on dynamics of the propagating waves are investigated. Furthermore, the simulated characteristics are compared with the numerical results. In addition, we report experimental observations of the several propagating waves.

2. Circuit setup

Figure 1(a) shows a schematic circuit diagram of a simple oscillator that is composed of one inductor (L), one capacitor (C), and one nonlinear conductance (NC). We assume that the voltage–current (v–i_{NC}) characteristics of the NC are given by the fifth-order polynomial

$$i_{NC} = g_1 v - g_3 v^3 + g_5 v^5, \quad g_1, g_3, g_5 > 0. \tag{1}$$

The NC operates as a passive resistor when a low voltage is applied to the oscillator. This results in a no-oscillation state (a stable focus). In contrast, when a high initial voltage is applied to C, the NC can produce a limit cycle oscillation. Because this oscillator has two steady-state: a stable focus and a limit cycle, the oscillator is called bistable oscillator.

In this paper, we assume that the six bistable oscillators are connected with an inductor (L_0), as shown in Fig. 1(b). The circuit equation of Fig. 1(b) is written as

$$\begin{aligned}&\frac{\mathrm{d}^2 v_k}{\mathrm{d}t^2} + \frac{g_1}{C}\left(1 - \frac{3g_3}{g_1}v_k^2 + \frac{5g_5}{g_1}v_k^4\right)\frac{\mathrm{d}v_k}{\mathrm{d}t} + \\ &\left(\frac{1}{LC} + \frac{1}{L_0 C}\right)v_k - \frac{1}{L_0 C}(v_{k+1} - v_k + v_{k-1}) = 0,\end{aligned} \tag{2}$$

$$k = 1, 2, \cdots 6 \quad (v_0 = v_6, v_7 = v_1).$$

Substituting

$$\begin{aligned}&t = \tau/\sqrt{(1/LC) + (1/L_0 C)}, \quad v_k = \sqrt[4]{g_1/5g_5}\, x_k, \\ &\varepsilon \equiv g_1/\sqrt{(C/L) + (C/L_0)}, \quad \alpha \equiv L/(L + L_0), \\ &\beta \equiv 3g_3/\sqrt{5g_1 g_5}, \qquad (\cdot = \mathrm{d}/\mathrm{d}\tau),\end{aligned} \tag{3}$$

into Eq. (2) yields the following normalized equation:

$$\begin{aligned}\dot{x}_k &= y_k, \\ \dot{y}_k &= -\varepsilon(1 - \beta x_k^2 + x_k^4)y_k \\ &\quad -(1-\alpha)x_k + \alpha(x_{k-1} - 2x_k + x_{k+1}).\end{aligned} \tag{4}$$

The parameter ε (> 0) indicates the degree of nonlinearity, whereas α ($0 \leqq \alpha \leqq 1$) is the coupling factor. The parameter β determines the amplitude of oscillation.

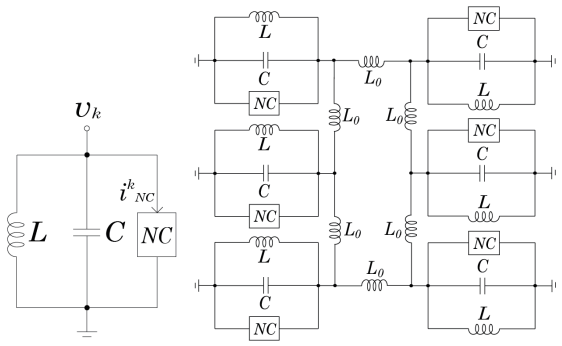

(a) Individual oscillator. (b) Circuit diagram.

Figure 1: Six-coupled bistable oscillators in a ring.

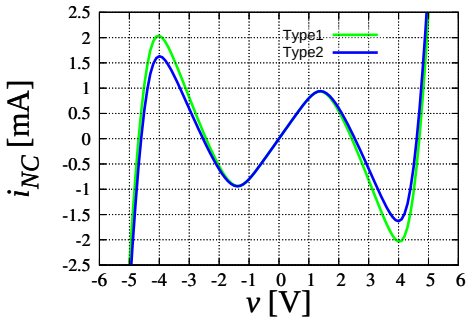

Figure 2: Two different characteristic curves for *NC*. The green and blue solid curves are called "type1" and "type2", respectively.

3. Results

From a viewpoint of circuit design, the voltage–current characteristic of *NC* plays a role in observing the propagating waves. First, we assume two different *NC*s, and investigate the influence on dynamics of the propagating waves by using LTSPICE. When we adopt one of *NC*s in the circuit experiment, it is shown that various propagating waves coexist.

3.1. SPICE simulation

Figure 2 shows two different *NC*s, which are obtained using LTSPICE. The two distinct characteristic curves are realized by changing the resistor values and the number of diodes in *NC*. The actual circuit for one of *NC*s is shown in [5]. We call two distinct *NC*s (the green and the blue curves) type1 and type2, respectively. In the following SPICE simulations, we use the same initial voltages such that $v_1 = 0.1$V, $v_2 = 0.05$ V, and the other $v_k = 0$. With both Type1 and type2, a propagating wave can be observed in the SPICE simulations when the element values are set appropriately. Figure 3 shows the time series

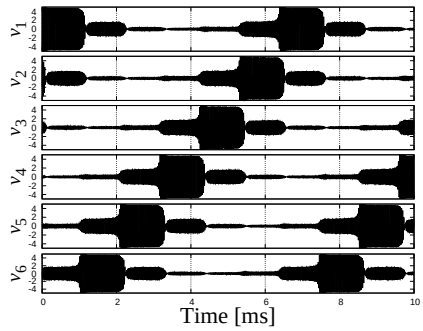

(a) Time series.

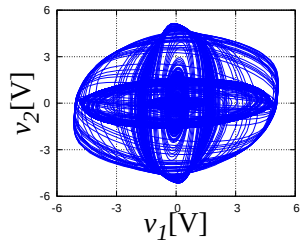

(b) Trajectory on the v_1–v_2 plane.

Figure 3: Propagating wave in SPICE simulation.

Table 1: Minimum and maximum values of L_0 in terms of C for type1 and type2.

	type1		type2	
C [nF]	L_0^s [mH]	L_0^l [mH]	L_0^s [mH]	L_0^l [mH]
8	4	14	5	9
10	4	17	4	13
12	4	18	4	15
14	4	20	4	17
16	3	21	4	18
18	3	22	4	19
20	3	24	4	20
22	3	25	4	21
24	3	27	4	22
26	3	27	4	23
28	3	27	4	25
30	3	28	4	26

of each voltage v_k, $k = 1, 2, \ldots, 6$, where the elements $L_0 = 20$ mH and $C = 14$ nF with Type1 are used. Table 1 gives the values of L_0 at which a propagating wave emerges (L_0^l) and disappears (L_0^s) as a function of C [1]. The difference ($L_0^l - L_0^s$) represents a existing regime of propagating wave phenomena. Comparing both cases where type1 and type2 are used, respectively, the existing regime of type1 is wider than that of type2. For $C > 30$nF, the value of L_0^l becomes larger.

To investigate the initiating points of the propagating waves in detail, we will compare the SPICE simulations with the numerical results of Eq.(4). Following the literatures [3, 4], a propagating wave emerges near a local (Pitch-fork; PF) bifurcation point of a limit cycle [2].

[1] Though there coexist several types of propagating waves, the type of the solutions is not identified at present.

[2] More precisely, a propagating wave comes from a global bifurcation

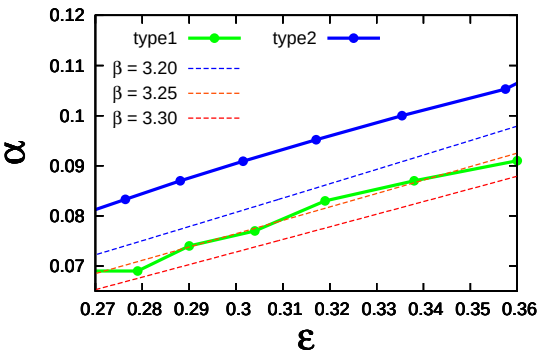

Figure 4: Two-parameter bifurcation diagram for three values of β in Eq. (4), and the simulated lines calculated by the values of L_0^l and C in Table 1.

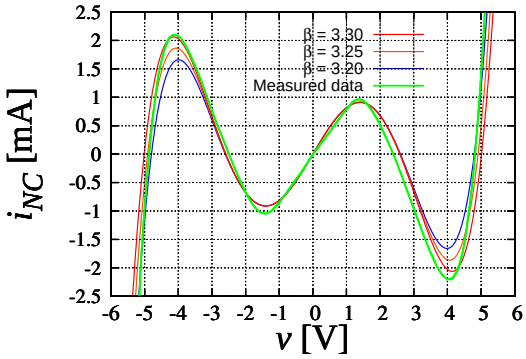

(a)

Figure 5: Experimentally measured voltage-current characteristics of the nonlinear conductance, and the fitting curves of Eq. (4) for three values of β.

The exact parameter values of the PF bifurcation point are numerically obtained using the procedure proposed by Kawakami [6], and we draw the two-parameter bifurcation diagram for three values of β using BUNKI. Note that the parameter β in Eq.(4) determines the voltage–current characteristic of NC. In addition, we calculate the parameter set (ε, α) using Eq. (3) from the values of C and L_0^l in Table 1, and the simulated results of type1 and type2 are superimposed in the numerical results, as shown in Fig. 4. The simulated line of type1 is consistent with the result for $\beta = 3.25$. In contrast, the simulated line of type2 is away from the numerical results for the three values of β.

3.2. Laboratory experiment

In this section, we concentrate on type1, and we investigate the propagating waves in the circuit experiments.

point, which is near the PF bifurcation point.

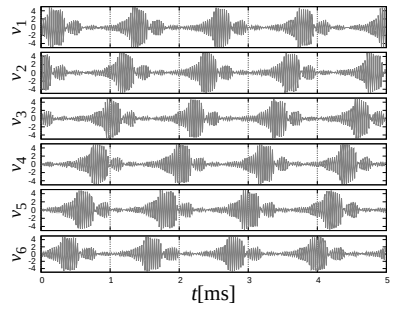

(a) Time series.

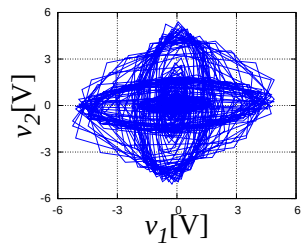

(b) Trajectory on the v_1–v_2 plane.

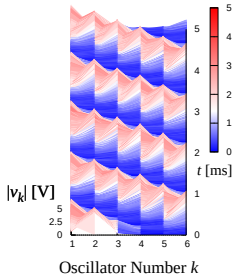

(c) 3D plot.

Figure 6: Experimentally obtained propagating wave (C = 15nF and L_0 = 14.3mH).

The experimentally measured curve of type1 and the characteristic curve obtained from Eq.(4) for three values of β are superimposed in Fig. 5. Though, at first glance, the measured curve of type1 agrees with the fit for $\beta = 3.3$, the simulated dynamics of the coupled oscillator system is consistent with the case of $\beta = 3.25$ as discussed in Sec.3.1. Therefore, it is considered that the voltage value of a breading point of the characteristic curve plays an important role in the observation of the propagating waves.

Figure 6 shows the experimental results using C = 15nF and L_0 = 14.3mH, where the time series of the voltages v_k, the trajectory on the v_1–v_2 plane, and 3D plot of $|v_k|$ are shown, respectively. It is clear that the quasi-periodic waves, which propagate in the oscillator array with constant speed, exists. When we assume $\beta = 3.25$, the corresponding parameter values are $\varepsilon = 0.342$ and $\alpha = 0.123$. It is remarkable that the qualitatively similar result is observed with the parameter set, as shown in Fig.7 (where Initial conditions are $x_1 = -0.7, x_2 = -0.1, x_3 = 0.1, x_4 = -0.1, x_5 = -1.0, x_6 = 0.6, y_1 = 0.2, y_2 = -0.1, y_3 = 0.0, y_4 = -0.2, y_5 = 0.3$, and $y_6 = 1.8$). In our previous work [5], we distinguished various propagating waves by comparing the trajectories on the phase planes. Although we failed to experimentally observe the propagating wave in the literature, we succeed in observing the propagating wave in the circuit experiment by using the slightly different NC. Moreover, Fig. 8 shows another propagating wave that is experimentally observed

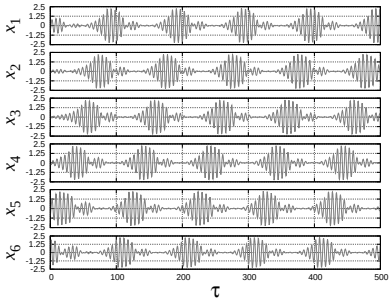

(a) Time series.

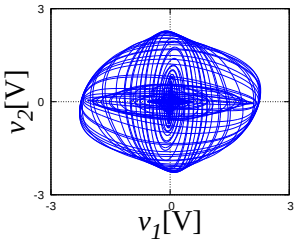

(b) Trajectory on the v_1–v_2 plane.

Figure 7: Numerical results corresponding to the propagating wave in Fig. 6 ($\alpha = 0.123, \beta = 3.25$, and $\varepsilon = 0.342$).

with the same parameter set. The associated numerical results can also be obtained (with the initial conditions: $x_1 = 2.0, x_2 = 0.5, x_3 = 0.1, x_4 = 0.2, x_5 = 0.9, x_6 = -2.2, y_1 = 1.8, y_2 = -0.3, y_3 = y_4 = 0.3, y_5 = -2.3$, and $y_6 = 0.4$), though no numerical results are presented due to space limitations.

4. Conclusions

This study performed an examination for the circuit implementation of the coupled bistable oscillators. By using a circuit simulator, we assumeed two different nonlinear conductances, and the influence on dynamics of the propagating waves were investigated. Furthermore, the simulated characteristics were compared with the numerical results. In addition, we reported experimental observations of the several propagating waves.

Acknowledgment

This study was supported in part by the MEXT-Supported Program for the Strategic Research Foundation at Private Universities 2013–2017 (s1311004).

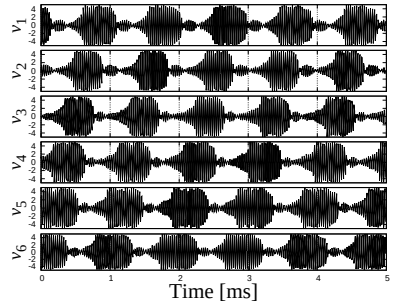

(a) Time series.

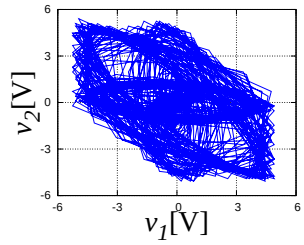

(b) Trajectory on the v_1–v_2 plane.

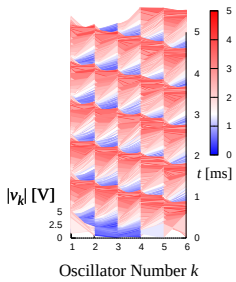

(c) 3D plot.

Figure 8: Experimentally obtained another propagating wave (C = 15nF and L_0 = 14.3mH).

References

[1] M. Sato, B. E. Hubbard, and A. J. Sievers, "Colloquim: Nonlinear energy localization and its manipulation in micro mechanical oscillator arrays," Reviews of Modern Physics, Vol.78, 2006.

[2] M. Kimura, and T. Hikihara, "Capture and release of traveling intrinsic localized mode in coupled cantilever array," Chaos, 19, 013138, 2009.

[3] K. Shimizu, M. Komuro, and T. Endo, "Onset of the propagating pulse wave in a ring of coupled bistable oscillators," Nonlinear Theory and Its Applications, IEICE, vol.2, no.1, pp.139–151, 2011.

[4] K. Kamiyama, M. Komuro, and T. Endo, "Bifurcation analysis of the propagating wave and the switching solutions in a ring of six-coupled bistable oscillators – bifurcation starting from type2 standing wave solution," Inter. Jour. of Bifurcation of Chaos, vol.22, no.5, 1250123, 2012.

[5] K. Shimizu, "Experimental observation of propagating waves and switching solutions in a coupled bistable oscillator system," Submitted to Int. Jour. Bifurcation Chaos.

[6] H. Kawakami, "Bifurcation of periodic responses in forced dynamic nonlinear circuits: computation of bifurcation values of the system parameters", IEEE Trans. Circuits Syst., vol.CAS-31, no.3, pp.248-260, 1984.